CHEMICAL ENGINEERING TRANSACTIONS
VOL. 116, 2025
A publication of AIDIC
The Italian Association of Chemical Engineering
Online at www.cetjournal.it
Guest Editors: Bruno Fabiano, Valerio Cozzani

ISBN 979-12-81206-18-2; **ISSN** 2283-9216
DOI: 10.3303/CET25116013

Determining Thermal Radiation from a Pool Fire using Computational Geometry

Mohammad Seyfi

Royal HaskoningDHV, Amersfoort, Netherlands
mohammad.seyfi@rhdhv.com

Determining the failure onset of an object due to incident thermal radiation from a fire has been a challenging topic in fire consequence analysis in the process safety industry. Failure of equipment exposed to fire is typically estimated using an uniform flame surface emissive power (SEP) in combination with atmospheric absorption and a view factor (configuration factor) which is usually determined based on the most conservative orientations and distances, namely the radiation target at the shortest distance and perpendicular to the incident radiation direction. The proposed method in this manuscript features a source-based representation of the view factor, as opposed to the conventional receiver-based view factors. This approach allows for a variable SEP instead of a uniform value for the entire flame region. The view factor is calculated using computational geometry, between individual segments of the radiation source and segments of the exposed object, based on analytical solutions of the view factor between finite surfaces. The total thermal radiation flux incident on each segment of the exposed object is thus calculated by summing the radiation from each fire segment using a separate SEP and view factor. To evaluate the proposed method with existing models, a simplified arrangement is considered. This involves a pool fire on the ground and a vertical cylindrical storage tank representing the exposed object. However, this method is applicable to a wide range of other spatial configurations, including multiple fire sources and exposed objects, as well as various shapes for flames or exposed objects.

1. Introduction

Domino effects and dynamic risk assessment have been addressed in many research papers with a focus on the probability of fire escalation via thermal load on nearby objects. Many studies are risk-based and use probit functions and the concept of time to failure (ttf). Several of these studies were summarized in the paper by Zhou et al. (2021). The proposed formulas for ttf in atmospheric and pressurized installations by Cozzani (2005) are frequently used in these studies. The fundamental assumption for such probit functions is that the target equipment which is exposed to fire effects is completely safe if mitigation measures can be in place before ttf (Jia et al., 2017). Despite their advantages for risk-based studies, probit functions have limitations for determining the failure onset of an exposed object based on its actual characteristics. Since probit functions consider the exposed object as a single equipment, it is not possible – to the knowledge of this author – to distinguish between different segments of an exposed object in terms of thermal load. In some cases, it is useful to estimate the time to failure based on the thermal load on different segments of an exposed object which is exposed to fire. For atmospheric storage tanks, an assessment by Amin et al. (2024) considered distinct regions for the exposed tank in contact with the liquid, the vapor, and the corresponding interface. It is thus worthwhile to obtain insights in the distribution of thermal load from a fire on different segments of an exposed object, without the need to carry out cumbersome calculations by Computational Fluid Dynamics (CFD). Although specific analysis of complicated situations, such as partial confinement and irregular geometries may only be possible with CFD analyses, simple analytical models for flame shapes may be sufficient when approximate results are more suitable (Palazzi and Fabiano, 2012) to quickly evaluate various arrangements and scenarios, especially during early stages of a new or modification project. The proposed method combines the advantage of simplified analyses, which require minimal input data, with the benefits of detailed analyses, which offer more refined and detailed results.

Paper Received: 2 December 2024; Revised: 1 March 2025; Accepted: 30 March 2025
Please cite this article as: Seyfi M., 2025, Determining Thermal Radiation from a Pool Fire Using Computational Geometry, Chemical Engineering Transactions, 116, 73-78 DOI:10.3303/CET25116013

This study utilizes computational geometry to provide a distribution of incident thermal radiation from different segments of flames perceived by different segments of an exposed object. As pool fires are among the most explored scenarios in literature (Fabiano et al., 2020), an application of the proposed method is presented based on a pool fire on the ground and a cylindrical vertical storage tank as the exposed object. The proposed model can also be applied to other situations including tank fires, jet fires (without flame impingement) and fireballs with multiple fire sources and exposed objects, and in general any arrangement where thermal load on an object is primarily by thermal radiation.

2. Methodology

The actual impact of a fire on an exposed object through thermal radiation is a function of the characteristics of the radiation emitting surface, atmospheric absorption, and the surface of the radiation receiving object. The proposed model considers a variable SEP along the flame height and provides the incident thermal radiation flux on each segment of the exposed object based on a summation of thermal radiation originating from different segments of the flame. Thus, a distribution is given for the incident thermal radiation flux on the exposed object. Figure 1 illustrates the main principles of the proposed method, as compared with conventional consequence modelling for thermal radiation.

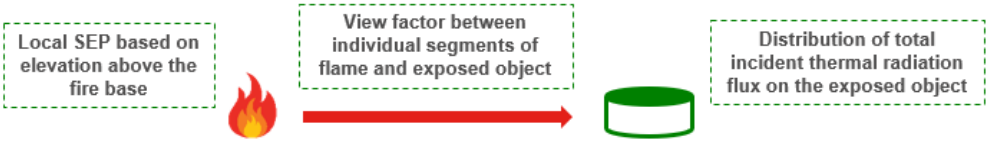

Figure 1: The proposed method for fire consequence modelling

2.1 Radiation from the pool fire

Conventional thermal radiation modelling generally uses the solid flame model, in which the flame region is represented by a cylinder, with dimensions determined by the flame base diameter, the visible flame height, and the flame tilt angle due to wind (Beyler, 2016). Several experimental studies demonstrate that the largest portion of the total thermal radiation from a large hydrocarbon pool fire is emitted from the flame region. Only this region is thus considered in this study as a [tilted] cylinder, although the same method can be applied to the smoke plume above the mean flame height.

In consequence modelling, an average SEP is typically considered either for the entire pool fire (single zone) or for the entire luminous and smoky regions (two zones) based on the fuel burning characteristics and the fire surface area (Xu, 2019). Both single-zone and two-zone models may be useful when considering fire effects on distant objects and observers. Yet, they may not be sufficient for short distances where the variation in SEP at different elevations can impact the incident radiation flux from different flame regions.

Since the emissive power from a pool fire is not entirely uniform over the flame surface area, a variable SEP is used in the proposed method for different segments of the pool fire based on the elevation from the pool. To focus on the differentiating aspects of this method, it is assumed that both radiation source and the exposed object act as gray surfaces, having no spectral and directional radiation dependencies (Howell et al., 2020). This is typically true for conventional thermal radiation modelling, except for some CFD studies. By neglecting the spectral and directional dependencies of thermal radiation intensity from any surface, the emissive power is the total rate of radiation emission per unit area of the radiation emitting surface, and the hemispherical emissive power is thus only dependent on the temperature of the radiation source (Howell et al., 2020). The general trend in temperature variation along the flame height is similar between large hydrocarbon pool fires and small pool fires (Beyler, 2016). For small pool fires, the temperature can be calculated based on the fire heat release rate, the flame shape, and the height above the base [of the virtual origin] of the pool fire. Semi-empirical correlations exist for the temperature along the centerline of small fire plumes, and similarly for the radial distribution of temperature based on the centerline temperature (Heskestad, 2016). However, thermal radiation trends from small pool fires cannot necessarily be used for large pool fires, which are the subject of interest in the process industry. Experimental studies have shown that the radiative fraction drops significantly with large pool diameters, primarily due to the obscuration effect of smoke and partial blocking of the radiation from the luminous flame region (Beyler, 2016). For the case study in this manuscript, a correlation is assumed for the empirically obtained data by Múnoz et al. (2004) for an average SEP at different elevations.

2.2 View factor

The view factor $F_{A_1-A_2}$ is, by definition, a fraction of the diffusely radiated energy leaving surface A_1 which is incident on surface A_2 (Howell et al., 2020). Several analytical solutions exist for the view factor between finite surfaces in specific configurations, though the direct application of such solutions to real geometries may not be practical, thus numerical integration may be necessary. To eliminate the need for numerical integration for the present case study, a rather simplified approach is adopted. The view factor is calculated based on the described form by Ehlert and Smith (1993) for two finite plates, as given in Eq(1), and shown in Figure 2a. Here, the finite areas A_1 and A_2 represent the flame and the exposed segments, respectively, as seen in Figure 2b.

$$F_{A_1-A_2} = \frac{1}{(x_2-x_1)(y_2-y_1)} \sum_{l=1}^{2}\sum_{k=1}^{2}\sum_{j=1}^{2}\sum_{i=1}^{2}(-1)^{(i+j+k+l)} G(x_i, y_j, \eta_k, \xi_l)$$

$$G = \frac{1}{2\pi}\left[(y-\eta)[(x-\xi)^2+d^2]^{\frac{1}{2}} \tan^{-1}\left\{\frac{y-\eta}{[(x-\xi)^2+d^2]^{\frac{1}{2}}}\right\}\right. \quad (1)$$

$$\left. + (x-\xi)[(y-\eta)^2+d^2]^{\frac{1}{2}} \tan^{-1}\left\{\frac{x-\xi}{[(y-\eta)^2+d^2]^{\frac{1}{2}}}\right\} - \frac{d^2}{2}\ln[(x-\xi)^2+(y-\eta)^2+d^2]\right]$$

Note that the view factor as described by Ehlert and Smith (1993) is applicable to parallel plates, while the flame and exposed segments in the present case study are not necessarily parallel. Since the radiation intensity is independent of the direction of emission for gray surfaces, the amount of radiation emitted by each flame segment that is intercepted by each exposed segment depends solely on the solid angle that the exposed segment occupies when viewed from the flame segment. It is the projected area that matters in radiative exchange, rather than the true surface area (Howell et al., 2020). Thus, the view factor from a flame segment to an exposed segment is approximated with the view factor between the projection of that flame segment onto a parallel plate with the exposed segment, forming the same solid angle. Such approximation is valid when these segments are sufficiently small compared to the distance between the fire and the exposed object. A suitable surface area needs to be determined which does not impact the distribution of incident thermal radiation flux. For the arrangements in the present case-studies, this was determined based on a sensitivity analysis.

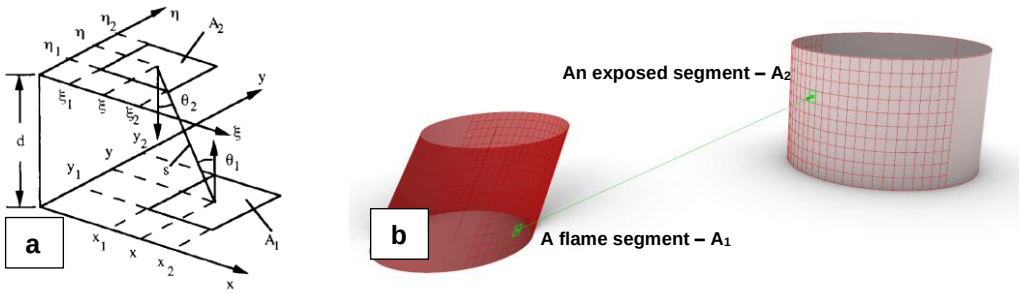

Figure 2. Arrangement of (a) parallel plates as given by Ehlert and Smith (1993), and (b) flame segments and exposed segments in the present study

2.1 Calculation of incident radiation flux distribution

The software Rhino Grasshopper® (McNeel et al., 2024) is used to calculate the view factor. Although this software is not originally purposed for such calculations, its capabilities in computational geometry are useful for calculating the view factor. An example is presented by Cabeza-Lainez et al. (2022) for calculating the view factor from a spherical fireball to a flat surface. For the present study, using computational geometry provides an immediate update of the incident thermal radiation flux distribution on the entire exposed object when adjusting input parameters such as the location and size of the pool fire and the exposed object, the wind speed and direction, and the fire characteristics of the flammable liquid. Here, the view factor is separately calculated between individual flame and exposed segments based on Eq(1) and using geometric inputs from Grasshopper. The total incident thermal radiation flux on each flame segment is then calculated as the sum of the radiation from each flame segment based on its SEP and view factor.

2.2 Application to a case study

To demonstrate the application of the proposed method, a gasoline pool fire is considered. The resulting incident thermal radiation flux is compared with existing view factor solutions as described by Beyler (2016) for simplified geometries, as well as radiation results of pool fire models using free-field consequence modelling, typically applied in the process industry. For the latter, a comparison is made with the commercial software PHAST™ (version 8.9) from DNV AS (2023). Note that the correlation as described by Beyler (2016) is only applicable to vertical fire plumes, while the pool fire modelling in PHAST is only applicable to tilted fire plumes, thus no direct comparison could be made between the two models. The present method is however applicable to both vertical and tilted fire plumes, and comparisons are thus made separately for each case.
To ensure consistency between the inputs for the mean flame height, the flame tilt angle and SEP, the empirical correlations and data from Múnoz et al. (2004) are used for these variables. However, the proposed method is independent of the specific model used for its inputs and can employ other correlations that may be more suitable for other arrangements. For the present case-studies, Eq(2) and Eq(3) are used for the mean flame height and the mean flame tilt angle (Múnoz et al., 2004). For parameters $\dot{m}"$ and $k\beta$, the values by Babrauskas (2016) are used for gasoline pools. The empirical data by Múnoz et al. (2004) is also used to determine SEP at each elevation, and a linear correlation is fitted to this experimental data. A more detailed description of the nomenclature can be found in Beyler (2016).

$$\frac{H}{D} = 7.74\,(m^*)^{0.375}(u^*)^{-0.096} \tag{2}$$

$$\cos\theta = 0.96(u^*)^{-0.26} \quad \text{for } u^* \geq 1 \qquad \text{or} \qquad \cos\theta = 1 \quad \text{for } u^* < 1 \tag{3}$$

Where:

$$m^* = \frac{\dot{m}"}{\rho_a\sqrt{gD}} \qquad u^* = \frac{u_w}{(g\dot{m}"D/\rho_a)^{\frac{1}{3}}} \qquad \dot{m}" = \dot{m}"_{\infty}\left(1 - e^{-k\beta D}\right)$$

3. Results and discussion

An example distribution of incident radiation heat flux on the exposed tank from a vertical or tilted pool fire using the proposed method is shown in Figure 3a and Figure 3b, respectively. The incident flux is evidently higher on the exposed segments at shorter distances and facing the fire plume. Since the segments on the sides of the exposed tank are 'seen' by a smaller number of flame segments, due to both the angle and the distance, the total incident radiation is significantly smaller for these segments. The closest exposed segments to the center of the pool fire are selected for comparing the results with the calculations using the described solution by Beyler (2016) and using PHAST. For simplicity of reading the results, the exposed tank is divided over 5 vertical segments, which are given by S1 to S5 in the remaining sections of this study.

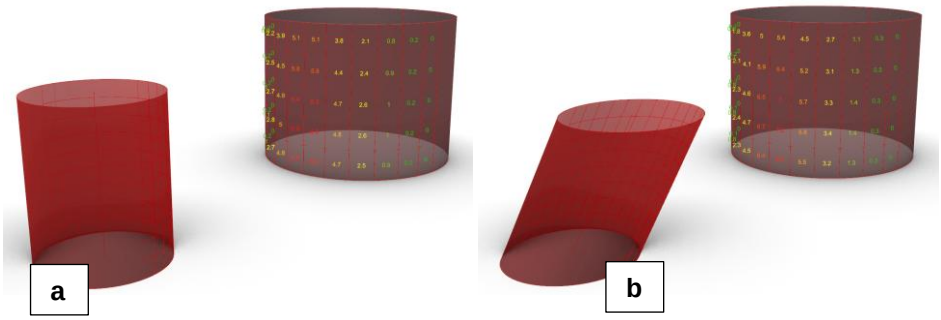

Figure 3. Distribution of incident thermal radiation flux on an exposed storage tank shell from (a) a vertical fire plume, and (b) a tilted fire plume, using the present method.

The method described by Beyler (2016) applies to vertical cylinders and calculates the view factor to a parallel target separately for each portion of the cylinder that falls below or above the exposed element. For a vertical fire plume, Figure 6 illustrates a comparison of results for exposed segments at different elevations at various horizontal distances, using both the present method and the method described by Beyler (2016). The relative differences between the two methods are summarized in Table 1. The present method predicts slightly more

conservative incident radiation flux values, ranging from 13% and 30% higher values compared to those obtained using the method by Beyler. Additionally, a similar impact from the elevation of the exposed segment on the total incident radiation is observed (seen Figure 4), thus a good agreement is found with the resulting values using descriptions by Beyler. Note that this comparison cannot be extended to other segments, as Beyler's method is not applicable to angled exposed surfaces.

For a tilted fire plume, the results from the present method are compared with those from consequence modelling in PHAST under weather condition 1.5/F and three wind directions with respect to the exposed tank: downwind (DW), in crosswind (CW) and upwind (UW). Since this [version of the] software does not have a dedicated substance for gasoline, n-octane is used as a representative substance. A comparison of relative difference between the results is summarized in Table 2. Results from the present method are in fair agreement but generally smaller than those obtained using PHAST, resulting in a negative deviation in several cases. These deviations can be attributed to different basic assumptions in the present method and the model in PHAST, such as the burning characteristics of gasoline (and n-octane), as well as the implemented correlations for modelling a tilted fire plume and atmospheric absorption. A variable SEP with height, which is not considered in PHAST (except only for two zones) plays a role and results in a higher incident radiation flux at lower segments of the exposed tank using the present method.

Table 1: Relative differences of incident thermal radiation flux from a vertical fire plume using the present method and the method described by Beyler (2016). Columns represent the horizontal distance.

Segment on exposed tank	5 m	10 m	15 m	20 m
S1	28%	21%	17%	15%
S2	30%	22%	17%	13%
S3	30%	22%	19%	13%
S4	29%	22%	17%	13%
S5	26%	20%	16%	14%

Table 2: Relative differences of incident thermal radiation flux from a tilted fire plume using the present method and using PHAST™. Columns represent the horizontal distance and wind direction.

Segment on exposed tank	10 m (DW)	15 m (DW)	20 m (DW)	10 m (CW)	15 m (CW)	20 m (CW)	10 m (UW)	15 m (UW)	20 m (UW)
S1	-35%	-37%	-33%	-2%	-17%	-18%	27%	13%	7%
S2	-34%	-35%	-33%	-9%	-17%	-21%	14%	4%	0%
S3	-37%	-33%	-30%	-17%	-20%	-25%	4%	-4%	-6%
S4	-41%	-34%	-33%	-25%	-22%	-25%	-9%	-7%	-6%
S5	-49%	-34%	-31%	-33%	-26%	-25%	-19%	-11%	-18%

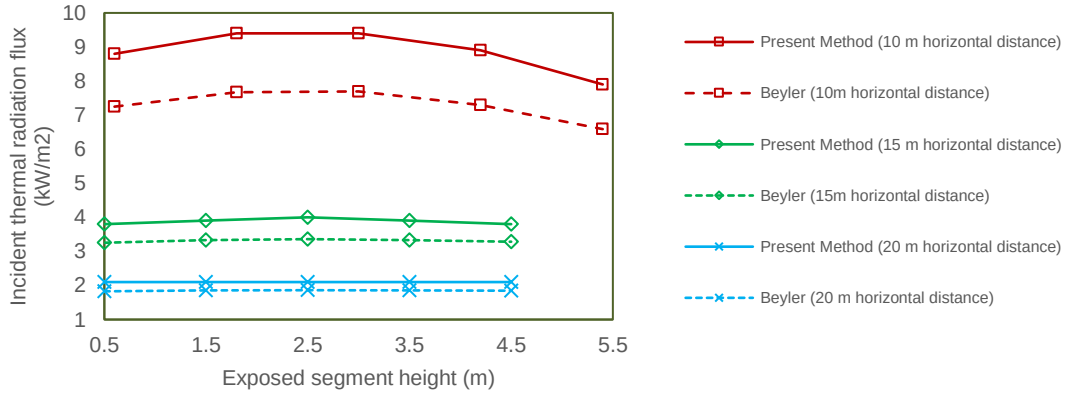

Figure 4. Comparison of incident thermal radiation flux from a vertical fire plume with the method described by Beyler (2016).

4. Conclusions

A method is proposed to determine the distribution of incident thermal radiation flux on typical equipment and installations in the process safety industry. This method calculates the incident radiation based on radiation emission from individual segments of the fire plume and the view factor from the fire source to the exposed object. This is opposed to the conventional approach which typically considers a uniform surface emissive power (SEP) and a view factor from the exposed object to the fire source. The radiation from individual fire segments is determined using the local SEP and existing solutions for view factors between two finite surfaces. Input variables for these calculations are derived using computational geometry, allowing results to be readily updated with any adjustments to input parameters, such as the pool fire characteristics and size, the locations and shapes of the flames and exposed objects. The proposed method is suitable for preliminary consequence analyses involving numerous scenarios yet also provides more refined results than conventional modelling regarding thermal radiation effects.

A pool fire and a cylindrical storage tank are considered as the case study to compare the results obtained using the present method with results obtained using geometric solutions for simplified geometries, as well as with results from common free-field consequence analyses in the process safety industry. A similar behavior is seen with both geometric solutions and free-field modelling regarding the total thermal radiation incident on exposed segments at different heights. The incident radiation flux obtained using the proposed method aligns well with those from geometric solutions for simple configurations, showing a relative difference of up to 30%. Results are also in good agreement with more practical free-field consequence modelling, with a relative difference of up to 40%. This difference is partly due to the adoption of a variable SEP in the proposed method and partly attributed to differing basic assumptions for representing input variables for calculations, such as atmospheric absorption and the mean flame height and tilt angle. However, the models adopted for these parameters are not intrinsic to the proposed method and are merely used for the case study.

Nomenclature

$F_{A_1-A_2}$ – View factor from A_1 to A_2
D – pool fire diameter, m
H – Flame height, m
SEP – Surface emissive power, W/m^2

References

Amin, M. T., Scarponi, G. E., Cozzani, V., Khan, F., 2024. Dynamic Domino Effect Assessment (D2EA) in tank farms using a machine learning-based approach. Computers & Chemical Engineering, 181, 108556.

Babrauskas, V., 2016. Heat release rates. In M. Hurley (Ed.), SFPE handbook of fire protection engineering (pp. 799-904). Springer.

Beyler, C. L., 2016. Fire Hazard Calculations for Large, Open Hydrocarbon Fires. In M. Hurley (Ed.), SFPE handbook of fire protection engineering (pp. 2591-2663). Springer.

Digital Solutions at DNV, 2023. PHAST™ (version 9.0) [Computer software]. DNV AS.

Cabeza-Lainez, J.M., Salguero-Andújar, F., Rodríguez-Cunill, I., 2022. Prevention of hazards induced by a radiation fireball through computational geometry and parametric design. Mathematics, 10(3), p.387.

Cozzani, V., Gubinelli, G., Antonioni, G., Spadoni, G., Zanelli, S., 2005. The assessment of risk caused by domino effect in quantitative area risk analysis. Journal of Hazardous Materials, 127(1–3), 14–30.

Fabiano B., Curro F., Reverberi A., 2020, Domino Effect by Pool Fire Radiation on Pipelines. an Applicative Case-study, Chemical Engineering Transactions, 82, 265-270.

Hollands, K. G. T., 1995. On the superposition rule for configuration factors.

Howell, J. R., Mengüç, M. P., Daun, K., Siegel, R., 2020. Thermal radiation heat transfer. CRC press.

Jia, M., Chen, G., Reniers, G., 2017. An innovative framework for determining the damage probability of equipment exposed to fire. Fire Safety Journal, 92, 177–187.

McNeel, R., & others., 2024. Rhino3d (Version 7.0) [Computer software]. Robert McNeel & Associates.

Muñoz, M., Arnaldos, J., Casal, J., Planas, E., 2004. Analysis of the geometric and radiative characteristics of hydrocarbon pool fires. Combustion and Flame, 139(3), 263-277.

Palazzi, E., Fabiano, B., 2012. Analytical modelling of hydrocarbon pool fires: Conservative evaluation of flame temperature and thermal power. Process Safety and Environmental Protection, 90(2), pp.121-128.

Sparrow, E. M., 1963. A new and simpler formulation for radiative angle factors.

Xu, Y., 2019. Theory pool fire model for Phast (version 8.7) [Software]. DNV GL

Zhou, J., Reniers, G., Cozzani, V., 2021. Improved probit models to assess equipment failure caused by domino effect accounting for dynamic and synergistic effects of multiple fires. Process Safety and Environmental Protection, 154, 306–314.